View metadata, citation and similar papers at core.ac.uk
brought to you by CORE
provided by UKM Journal Article Repository

Sains Malaysiana 43(6)(2014): 923–927

Structural Properties of Zinc Oxide Thin Films Deposited on Various Substrates
(Ciri Struktur Filem Nipis Zink Oksida yang Dimendapkan di atas Substrat Berlainan)

C.G. CHING*, P.K. OOI, S.S. NG, Z. HASSAN, H. ABU HASSAN & M.J. ABDULLAH

ABSTRACT

In this work, the structural properties of radio frequency sputtering-grown zinc oxide (ZnO) thin films on sapphire (Al_2O_3), gallium arsenide (GaAs) and n-type silicon (Si) substrates were characterized. Scanning electron microscopy was employed to study the surface morphology of the samples. X-ray diffraction (XRD) measurements were also performed to obtain the structural information of the samples. The XRD results showed that the ZnO layers grown on different substrates have similar lattice constant (c) values, which were used to calculate the strain percentages of the ZnO thin films. The surface morphologies of the ZnO thin films indicated the formation of a granular surface when ZnO is deposited on n-type Si(100) and Si(111) substrates. Meanwhile, a leaf-like surface is obtained when ZnO is deposited on GaAs and Al_2O_3 substrates. The results showed that the ZnO thin film grown on n-type Si(100) has the best quality among all the samples.

Keywords: Gallium arsenide; sapphire; silicon; XRD; zinc oxide

ABSTRAK

Dalam kajian ini, pencirian struktur filem nipis zink oksida (ZnO) yang ditumbuhkan dengan teknik percikan frekuensi radio ke atas substrat nilam (Al_2O_3), galium arsenik (GaAs) dan silikon (Si) jenis-n telah dijalankan. Mikroskop elektron imbasan digunakan untuk memperoleh morfologi permukaan sampel manakala pembelauan sinar-X (XRD) pula digunakan untuk memperoleh maklumat struktur bagi sampel. Keputusan XRD menunjukkan ZnO yang ditumbuhkan di atas substrat berlainan mempunyai pemalar kekisi paksi-c yang hampir sama. Nilai pemalar kekisi paksi-c yang diperoleh digunakan untuk menghitung peratusan ketegangan filem nipis ZnO. Morfologi permukaan filem nipis ZnO menunjukkan pembentukan permukaan bercorak butiran apabila ZnO ditumbuhkan ke atas substrat Si(100) dan Si(111) jenis-n dan permukaan bercorak daun diperoleh apabila ZnO ditumbuhkan ke atas substrat GaAs dan Al_2O_3. Akhirnya, keputusan XRD menunjukkan bahawa filem nipis yang ditumbuhkan ke atas Si(100) jenis-n mempunyai kualiti kristal yang terbaik antara sampel.

Kata kunci: Galium arsenida; nilam; pembelauan sinar-X; silikon; zink oksida

INTRODUCTION

The recent utilization of zinc oxide (ZnO) materials in the fabrication of devices has increased research interest in the properties of these materials. The unique characteristics of ZnO, such as a wide bandgap energy of ~3.37 eV (Ashrafi et al. 2004) and high exciton-binding energy of ~60 meV (Jeon et al. 2007; Matsumoto et al. 2004) made them suitable in various applications, including light-emitting diodes (Ashrafi et al. 2005; Kim et al. 2008), sensors (Bie et al. 2007), field effect transistors (Ryu et al. 2005), and heterojunction and homojunction diodes (Kumar et al. 2010). ZnO has also enhanced chemical and thermal stabilities and a high mechanical strength (Ma et al. 2005). Thus, ZnO-based devices are durable enough to withstand rough operating environments.

ZnO epitaxial layers can be deposited on substrates by various deposition methods, including molecular beam epitaxy (MBE), metal organic chemical vapor deposition (MOCVD), spray pyrolisis, sol-gel method, atmospheric pressure vapor phase epitaxy, pulse laser deposition and radio frequency (RF) sputtering (Chang et al. 2005; Yang et al. 2010). Complex deposition methods, such as MBE and MOCVD can produce good-quality ZnO thin films. However, deposition is relatively expensive. Simpler methods like spray pyrolisis and the sol-gel method may require relatively lower costs but produce lower-quality thin films. By contrast, RF sputtering is a deposition method with a more moderate cost and average-quality thin films.

The types of substrates frequently used for ZnO thin film deposition include sapphire (Al_2O_3) (Iwata et al. 2000), silicon carbide (SiC) (Jeon et al. 2007), silicon (Si) (Kim et al. 2007) and gallium arsenide (GaAs) (Matsumoto et al. 2004). ZnO thin films grown on different substrates have different structural properties and surface morphologies. For instance, the thermal mismatch, crystallite size, crystalline quality and crystalline structure of ZnO varied when it was deposited on different substrates. This information is crucial in selecting the most appropriate substrate for the deposition of ZnO thin films for device fabrication.

The objective of this work was to investigate the structural properties and surface morphologies of ZnO thin films grown on various types of substrates (i.e. Al_2O_3, Si

and GaAs). Structural changes were evaluated by X-ray diffraction (XRD). The surface morphologies of the samples were assessed by scanning electron microscopy (SEM).

EXPERIMENTAL DETAILS

ZnO thin films were simultaneously deposited on Al_2O_3, GaAs, n-type Si(100) and n-type Si(111) substrates. The samples were deposited through an Edwards A500 RF sputtering system. The ZnO target with diameter of 76.2 mm with ~99.99% purity is used. The substrates were placed approximately 10 cm above the target. The sputter chamber was vacuumed until a pressure of approximately 5.0×10^{-5} mbar was achieved. High-purity (5N) argon (Ar) gas was introduced into the chamber. Afterwards, the target was pre-sputtered for approximately 10 min under a constant pressure of 2.0×10^{-2} mbar. ZnO thin films were deposited with the RF power of 200 W for 3 h.

The deposited ZnO thin films were characterized by XRD and SEM to assess their crystalline structure and surface morphology. All XRD measurements were performed through PanAlytical X'pert Pro MRD system with CuK_{a1} and CuK_{a2} X-ray sources. The X'pert Pro Highscore Plus software was used to analyzed the XRD patterns. Conventional phase analysis (PA) with scan range of 30° to 80° was used. Under this scan mode, the omega (ω) and 2theta (2q) axes were moved together to ensure only the diffracted beams from the crystalline planes parallel to the sample surface were detected. The information extracted from the XRD patterns were used to calculate the crystallite size and lattice constants. SEM imaging is performed through a JSM6460LV SEM (Jeol, Inc.). The samples for SEM were measured at an acceleration voltage of 10 kV at 10 000× magnification.

RESULTS AND DISCUSSION

Figure 1 shows the XRD-PA patterns of ZnO grown on the Al_2O_3, GaAs, n-Si(100) and n-Si(111) substrates, which were labeled as samples A, B, C and D, respectively. All ZnO peaks observed were defined as the wurtzite structure of ZnO. The XRD spectra of all samples were dominated by ZnO(002), located from 34.2° to 34.4°. The XRD spectra indicate that ZnO thin films with wurtzite structure have been successfully grown by RF sputtering. Aside from ZnO(002), the peaks that were ascribed to other phases of ZnO were also observed in all samples. Thus, the ZnO thin films deposited in this study have multiple-phase origins. Peaks corresponding to the substrates were also observed in the XRD-PA patterns.

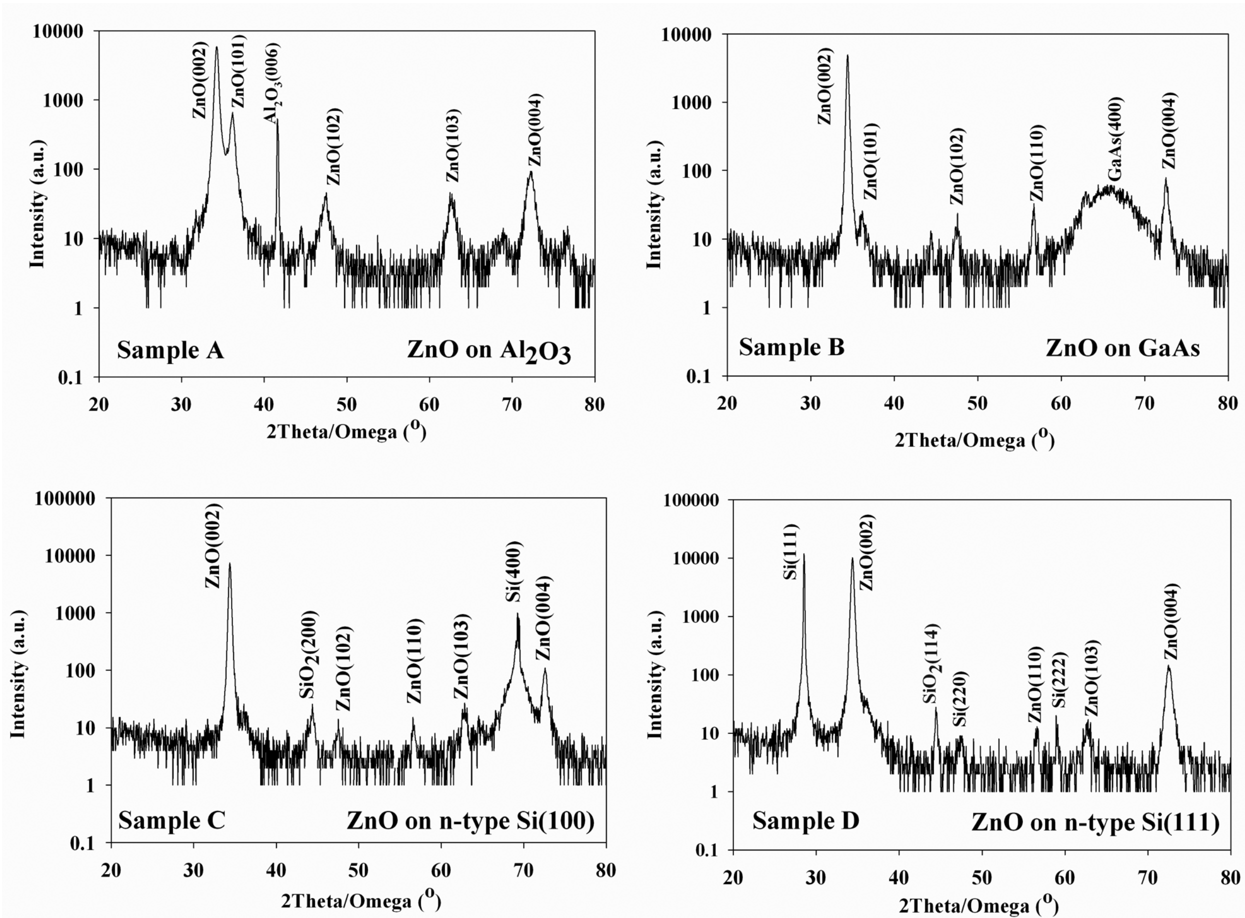

FIGURE 1. XRD-PA patterns of ZnO thin films grown on various substrates

Table 1 shows a brief summary of the structural information extracted from the XRD-PA spectra. The peak position of ZnO(002) slightly varies across the samples. The variation in peak position may be due to the different strain levels in the sample. The strain was attributed to the lattice mismatch between the ZnO thin films and substrates (Kang et al. 2010; Lee et al. 2009). Furthermore, the full width half maximum (FWHM) values of the ZnO thin film deposited on n-type Si(100) (sample C) and GaAs (sample B) was relatively low (~14.4 arc min.) compared with other samples in this work. These results showed that these ZnO thin films have a relatively higher crystalline quality compared with the other samples. Considering the peak intensity in the XRD-PA spectra, the intensity of the ZnO(002) peak in sample C (7220 counts) is higher than that in sample B (4884 counts). Thus, the crystalline quality of the ZnO thin film in sample C is higher than that of sample B. The intensities of the XRD peaks were compared, assuming that the thicknesses of the ZnO thin films of all the samples were the same because they were deposited at the same time through the same RF sputtering system. Therefore, only thin films with a higher crystalline quality allow a higher X-ray intensity to be reflected back to the detector.

The information extracted from the XRD spectra were used to calculate the lattice constant *c*, as well as the crystallite size, of the ZnO. The lattice constant *c* for any allowed (000*l*), in our case, the ZnO(0002) peak, is calculated through the equation below:

$$c = \frac{l\lambda}{2\sin\theta}, \quad (1)$$

where *l* is the Miller indices, l is the wavelength of the X-ray source used (l = 1.5406 for the K_{a1} line) and q is the diffracted angle or the half value of the position (in 2q) of a particular peak. This formula is only applicable to peaks that were assigned to the phase in the (000*l*) form. The crystallite sizes were calculated through Scherer's equation (Choudhury & Sarma 2009):

$$D_p = \frac{k\lambda}{\beta\cos\theta}, \quad (2)$$

where *k* is the Scherer's constant (value used is 0.94) and b is the FWHM of the related peak. The strain along the *c*-axis in the samples was calculated through the following equation (Kang et al. 2010):

$$\varepsilon_{zz} = \frac{c - c_o}{c_o} \times 100\%. \quad (3)$$

where c_o is the unstrained lattice constant with the value of 5.207 Å, as reported by Kang et al. (2010) and *c* is the lattice constant that was obtained experimentally.

The calculated results were presented in Table 1. The lattice constant *c* values of the ZnO layers of the samples were relatively close to one another and similar to the values reported by Chang et al. (2005). The calculation performed through Scherrer's equation showed that samples B and C had the largest crystallite sizes. The FWHM of the peaks were inversely proportional to crystallite size. In other words, the bigger the crystallite size of the ZnO thin films, the better the crystalline quality. The strain percentage in the ZnO thin film samples B, C and D were relatively smaller, which indicates that the thin films were in an almost relaxed state. The highest strain percentages were observed in ZnO thin films deposited on Al_2O_3, which may have contributed to the relatively larger shift of the ZnO(002) peak in sample A. The positive strain percentages in all the samples signified tensile strain.

Figure 2 shows the SEM images of ZnO grown on different substrates. Uniform distributions of ZnO grains on the substrates without any ZnO islands were obtained. However, samples C and D show different surface morphologies compared with samples A and B. The ZnO layers deposited for samples C and D show granular surfaces, whereas those for samples A and B have leaf-like grains. A similar granular surface morphology shown in the SEM images of samples C and D was reported by Schuler et al. (2005). A leaf-like grain shape was also reported by Hung et al. (2008). The variation in the surface morphology of the samples is attributed to the lattice mismatch and surface conditions of the substrates (Hung et al. 2008). The surface morphological changes were also ascribed to other factors, such as chemical bonding across the interface and the presence of residual oxides (Talla et al. 2010). In the present case, given that the growing parameters and temperature of the ZnO thin films on the substrates were

TABLE 1. Structural information on ZnO thin films grown on various substrates extracted from the XRD-PA pattern

Sample	Substrate	ZnO Peak Position (°)	FWHM [ZnO(002) peaks, arc min]	ZnO Lattice constant *c* (Å)	Crystallite Size (Å)	Strain (%)
a	Al_2O_3	34.25	22.8	5.23	23	0.44
b	GaAs	34.41	14.4	5.21	36	0.06
c	n-type Si(100)	34.38	14.4	5.21	36	0.06
d	n-type Si(111)	34.38	17.4	5.21	30	0.06

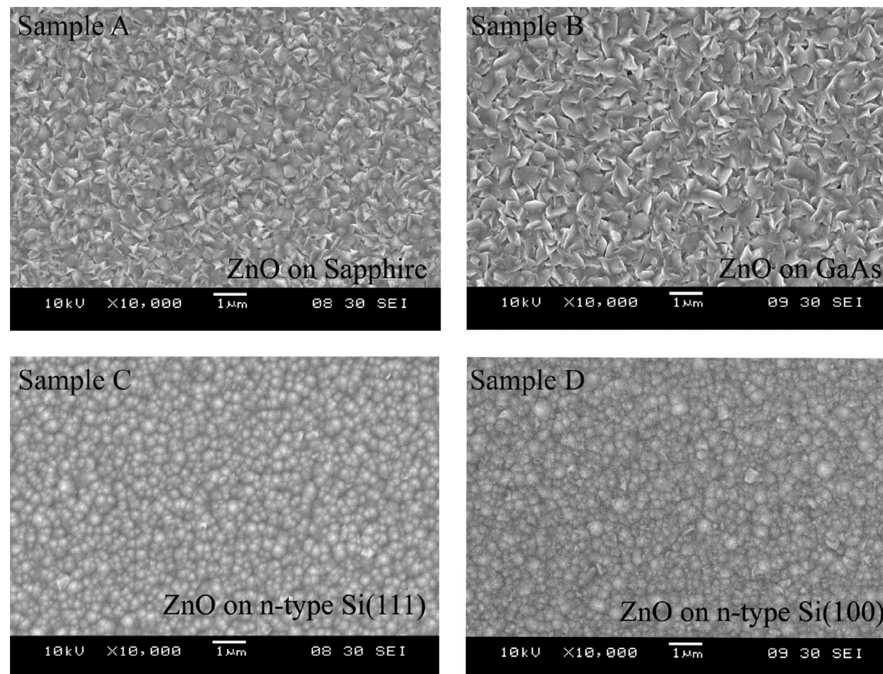

FIGURE 2. Surface morphology of ZnO thin films deposited on various substrates

the same, we strongly believe that the surface conditions of the substrate and chemical bonding in the substrate–layer interface were the main factors causing the changes in the surface morphology of the samples.

CONCLUSION

The effects of substrate type on the structural properties of the ZnO epilayers were investigated via XRD-PA and SEM. The XRD-PA results showed that the wurtzite structure of the ZnO epilayers can be successfully grown on n-Si(100), n-Si(111), GaAs, and Al_2O_3 substrates by RF sputtering. Analysis of the XRD-PA patterns showed that samples C and D had a relatively higher crystalline quality. Based on the ZnO(002) peak intensity, the crystalline quality of sample C was higher than that of sample B. XRD-PA also showed that the lattice constant *c* of the samples is around 5.2 Å. The crystallite size of the samples ranged from 20 to 37 Å, which also indicate a good crystallinity of the samples. The calculation of the strain percentage indicated the presence of tensile strain in all ZnO thin films. Similar strain percentage values were obtained for samples B, C and D. The highest strain percentage was observed in sample A. The SEM images showed that samples C and D had a granular surface, whereas the other samples had a leaf-like surface. Finally, the characterization results showed that ZnO deposited on n-Si(100) (sample C) has the highest crystalline quality among the samples.

ACKNOWLEDGEMENTS

The authors were grateful for the support given by the Universiti Sains Malaysia through the Short Term Grant (Account No.: 304/PFIZIK/6311014) and Postgraduate Research Grant Scheme (Account No.: 1001/PFIZIK/834090).

REFERENCES

Ashrafi, A.B.M.A., Zhang, B.P., Binh, N.T., Wakatsuki, K. & Segawa, Y. 2005. Biaxial strain effect in exciton resonance energies of epitaxial ZnO layers grown on 6H–SiC substrates. *J. Cryst. Growth* 275: e2439-e2443.

Ashrafi, A.B.M.A., Zhang, B.P., Nguyen, B.T. & Segawa, Y. 2004. High-quality ZnO layers grown on 6H-SiC substrates. *Jpn. J. Appl. Phys*. 43: 1114-1117.

Bie, L.J., Yan, X.N., Yin, J., Duan, Y.Q. & Yuan, Z.H. 2007. Nanopillar ZnO gas sensor for hydrogen and ethanol. *Sensor Actuat. B-Chem*. 126: 604-608.

Chang, R.C., Chu, S.Y., Lo, K.Y., Lo, S.C. & Huang, Y.R. 2005. Physical and structural properties of RF magnetron sputtered ZnO films. *Integr. Ferroelectr*. 69: 43-53.

Choudhury, N. & Sarma, B.K. 2009. Structural characterization of lead sulfide thin films by means of X-ray line profile analysis. *Bull. Mater. Sci*. 32: 43-47.

Hung, S.C., Huang, P.J., Chan, C.E., Uen, W.Y., Ren, F., Pearton, S.J., Yang, T.N., Chiang, C.C., Lan, S.M. & Chi, G.C. 2008. Nanostructured surface morphology of ZnO grown on p-type GaN and Si by metal organic chemical vapor deposition. *Appl. Surf. Sci*. 255: 3016-3018.

Iwata, K., Fons, P., Yamada, A., Matsubara, K. & Niki, S. 2000. Nitrogen-induced defects in ZnO: N grown on sapphire substrate by gas source MBE. *J. Cryst. Growth* 209: 526-531.

Jeon, Y.S., Kim, D.M. & Hwang, K.S. 2007. Epitaxially grown ZnO thin films on 6H-SiC(0001) substrates prepared by spin coating-pyrolysis. *Appl. Surf. Sci*. 253: 7016-7018.

Kang, M.I., Kim, S.W., Kim, Y.G. & Ryu, J.W. 2010. Dependence of the optical anisotropy of ZnO thin films on the structural properties. *J. Korean Phys. Soc*. 57: 389-394.

Kim, E.H., Lee, D.H., Chung, B.H., Kim, H.S., Kim, Y. & Noh, S.J. 2007. Low-temperature growth of ZnO thin films by atomic layer deposition. *J. Korean Phys. Soc*. 50: 1716-1718.

Kim, J.B., Byun, D., Ie, S.Y., Park, D.H., Choi, W.K., Choi, J.W. & Angadi, B. 2008. Cu-doped ZnO-based p–n hetero-junction light emitting diode. *Semicond. Sci. Tech*. 23: 095004.

Kumar, M., Kar, J.P., Kim, I.S., Choi, S.Y. & Myoung, J.M. 2010. Growth of p-type ZnO thin film on n-type silicon substrate and its application as hybrid homojunction. *Curr. Appl. Phys*. 11: 65-69.

Lee, J.H., Kim, Y.Y., Cho, H.K. & Lee, J.Y. 2009. Microstructural characteristics and crystallographic evolutions of Ga-doped ZnO films grown on sapphire substrates at high temperatures by RF magnetron sputtering. *J. Cryst. Growth* 311: 4641-4646.

Ma, Y., Du, G., Yin, J., Yang, T. & Zhang, Y. 2005. Structural and optoelectrical properties of ZnO thin films deposited on GaAs substrate by metal-organic chemical vapour deposition (MOCVD). *Semicond. Sci. Technol*. 20: 1198-1202.

Matsumoto, T., Nishimura, K., Nabetani, Y. & Kato, T. 2004. MBE growth and optical properties of ZnO on GaAs(111) substrates. *Phys. Stat. Sol. (b)* 241: 591-594.

Ryu, Y.R., Lee, T.S., Lubguban, J.A., White, H.W., Park, Y.S. & Youn, C.J. 2005. ZnO devices: Photodiodes and p-type field-effect transistors. *Appl. Phys. Lett*. 87: 153504.

Schuler, L.P., Alkaisi, M.M., Miller, P., Reeves, R.J. & Markwitz, A. 2005. Comparison of DC and RF sputtered zinc oxide films with post-annealing and dry etching and effect on crystal composition. *Jpn. J. Appl. Phys*. 44: 7555-7560.

Talla, K., Dangbégnon, J.K., Wagener, M.C. & Botha, J.R. 2010. ZnO grown by metal organic chemical vapor deposition: Effect of substrate on optical and structural properties. *South African Institute of Electrical Engineers* 101: 37-41.

Yang, X.L., Chen, N.F., Yin, Z.G., Zhang, X.W., Li, Y., You, J.B., Wang, Y., Dong, J.J., Cui, M., Gao, Y., Huang, T.M., Chen, X.F. & Wang, Y.S. 2010. Epitaxial growth of ZnO on GaN/sapphire substrate by radio-frequency magnetron sputtering. *J. Semicond*. 31: 093001.

Nano-Optoelectronics Research and Technology Laboratory
School of Physics, Universiti Sains Malaysia
11800 Penang
Malaysia

*Corresponding author; email: chingchinguan@gmail.com

Received: 2 March 2013
Accepted: 26 January 2014